Hindawi Publishing Corporation
International Journal of Microwave Science and Technology
Volume 2014, Article ID 849194, 8 pages
http://dx.doi.org/10.1155/2014/849194

*Research Article*

# A New Method of Designing Circularly Symmetric Shaped Dual Reflector Antennas Using Distorted Conics

**Mohammad Asif Zaman and Md. Abdul Matin**

*Department of Electrical and Electronic Engineering, Bangladesh University of Engineering and Technology, Dhaka 1000, Bangladesh*

Correspondence should be addressed to Mohammad Asif Zaman; asifzaman13@gmail.com

Received 30 July 2014; Accepted 1 December 2014; Published 17 December 2014

Academic Editor: Ramon Gonzalo



A new method of designing circularly symmetric shaped dual reflector antennas using distorted conics is presented. The surface of the shaped subreflector is expressed using a new set of equations employing differential geometry. The proposed equations require only a small number of parameters to accurately describe practical shaped subreflector surfaces. A geometrical optics (GO) based method is used to synthesize the shaped main reflector surface corresponding to the shaped subreflector. Using the proposed method, a shaped Cassegrain dual reflector system is designed. The field scattered from the subreflector is calculated using uniform geometrical theory of diffraction (UTD). Finally, a numerical example is provided showing how a shaped subreflector produces more uniform illumination over the main reflector aperture compared to an unshaped subreflector.

## 1. Introduction

Reflector antennas are widely used in radars, radio astronomy, satellite communication and tracking, remote sensing, deep space communication, microwave and millimetre wave communications, and so forth [1–3]. The rapid developments in these fields have created demands for development of sophisticated reflector antenna configurations. There is also a corresponding demand for analytical, numerical, and experimental methods of design and analysis techniques of such antennas.

The configuration of the reflectors depends heavily on the application. The dual reflector antennas are preferred in many applications because they allow convenient positioning of the feed antenna near the vertex of the main reflector and positioning of other bulky types of equipment behind the main reflector [3]. Also, the feed waveguide length is reduced [4]. They also have some significant electromagnetic advantage over single reflector systems [5]. Although many dual reflector configurations exist, the circularly symmetric dual reflector antennas remain one of the most popular choices for numerous applications [1].

One of the most common circularly symmetric dual reflector antennas is the Cassegrain antenna. The Cassegrain antenna is composed of a hyperboloidal subreflector and a paraboloidal main reflector. A feed antenna (usually a horn antenna) illuminates the subreflector which in turn illuminates the main reflector. The main reflector produces the radiated electric field that propagates into space. The radiation performance of the dual reflector antennas depends on the radiation characteristics of the feed and the geometrical shapes of the main reflector and the subreflector. Modern wireless communication and RADAR applications enforce stringent requirements on the far-field characteristics of the antenna. For example, satellite communications impose limitations on maximum beamwidth and maximum sidelobe levels of the antenna to avoid interference with adjacent satellites [2]. The traditional Cassegrain antennas have fixed geometries and offer limited flexibilities to antenna designers. As a result, the maximum performance that can be extracted from these antennas is limited by geometrical constraints.

For high performance applications, the traditional hyperboloid/paraboloidal geometry must be changed. Reflector shaping is the method of changing the shape of the reflecting

surfaces to improve the performance of the antenna. Shaped reflector antennas outperform conventional unshaped reflector antennas. Reflector shaping allows the designers additional flexibility. The antenna designers have independent control over relative position of the reflectors, diameter of the reflectors, and the curvature of the reflectors when shaped reflectors are used instead of conventional reflectors. This makes reflector shaping an essential tool for designing high performance reflector antennas.

Many methods of designing shaped reflectors are present in literature. One of the first major articles related to reflector shaping was published by Galindo in 1964 [6]. The method is based on geometrical optics (GO). Galindo's method required solution of multiple nonlinear differential equations, which sometimes may be computationally demanding. A modified version of this method was presented by Lee [7]. Lee divided the reflector surfaces into small sections and assumed the sections to be locally planar. This assumption converted the differential equations to algebraic equations, which are much easier to solve. However, the reflector surface must be divided into a large number of sections to increase the accuracy of this method.

Another popular method for designing shaped reflectors involves expanding the shaped surfaces using a set of orthogonal basis functions [8, 9]. Rahmat-Samii has published multiple research papers on this area [8–10]. The expansion coefficients determine the shape of the surface. A small number of terms of the expansion set are sufficient to accurately describe a shaped surface. So, a few expansion coefficients must be determined to define the surface. The differential equation based methods determine the coordinates of the points on the reflector surfaces, whereas the surface expansion based method only determines the expansion coefficients. Due to the decrease in number of unknowns, the surface expansion method is computationally less demanding. The surface expansion method can be incorporated with geometrical theory of diffraction (GTD) or its uniform version, uniform theory of diffraction (UTD), to produce an accurate design algorithm [10]. These design procedures are known as diffraction synthesis [8–10]. This method has been successfully used in many applications. Recently, a few new efficient methods for designing circularly symmetric shaped dual reflector design have been developed. One of the first significant works on this method was reported by Kim and Lee in 2009 [11]. This method divides the shaped reflector surfaces into electrically small sections. Each section is assumed to be a conventional unshaped dual reflector system. Since well-established methods for analyzing conventional dual reflector system exist, the radiation characteristics of each section can easily be evaluated. The shaped surface is defined by combining all the local conventional surfaces. The method requires solutions of several nonlinear algebraic equations. So it is computationally convenient. Another method based on the same principle was proposed by Moreira and Bergmann in 2011 [12]. This method also divides the shaped surface into small local sections. The local sections are represented by unshaped conics. Each conic section is optimized to produce a desired aperture distribution, which is formulated by GO method. As these methods have recently appeared in literature, most of the advantages and drawbacks of the method have not been investigated. Reduction in computational complexity is an obvious advantage. The proposed work concentrated on presenting an alternative method rather than improving the existing methods.

A design method that requires lesser number of parameters to define the shaped reflector surfaces without decreasing accuracy of the obtained results is a challenging goal for reflector antenna designers. In this paper, the surface of the shaped reflector is defined using a novel equation. The shaped subreflector surfaces are assumed to be distorted forms of unshaped surfaces. As most shaped subreflectors resemble their unshaped counterparts [11–13], the assumption is logical. The shaped surfaces can therefore be represented by modified versions of the equations that represent the conventional unshaped surfaces. This method of visualizing the shaped surface as perturbed/distorted form of unshaped surface has not been reported in literature yet. As the general form of the surface is generated from the conventional conics, only a small number of parameters need be used to represent the shaped surface. Once the subreflector surface is defined, the main reflector surface is defined using GO method and equal optical path length criterion.

The paper is organized as follows. Section 2 describes the geometry of the shaped subreflector. Surface equations and differential geometric analysis are presented in this section. The synthesis method of the main reflector is discussed in Section 3. Section 4 covers the numerical results. Concluding remarks are made in Section 5.

## 2. Geometry of the Shaped Subreflector

*2.1. Surface Equations.* In a conventional Cassegrain geometry, the subreflector is hyperboloidal. In shaped-Cassegrain geometry, the subreflector is shaped to provide a desired illumination over the aperture of the main reflector. However, the geometrical features of this shaped subreflector are very similar to the geometrical features of the unshaped hyperboloid. Due to these similarities, the shaped surfaces can be considered a distorted form of the unshaped surfaces. So, to define the geometry of the shaped subreflector, the conventional Cassegrain geometry must be described first.

The geometry of a Cassegrain dual reflector antenna is shown in Figure 1. The parameters describing the geometry of the Cassegrain system are

$d_p$: diameter of the main reflector = 10 m,

$f_p$: focal length of the main reflector = 5 m,

$d_s$: diameter of the subreflector = 1.25 m,

$2c$: distance between the foci = 4 m,

$e$ = c/a: subreflector eccentricity = 1.4261,

$\Delta_p$: depth of the paraboloid = 1.25 m,

$l_p$: distance from feed to paraboloid vertex = 1 m,

$\psi_o$, $\phi_o$: opening half angle of the main reflector and subreflector = 53.13° and 10.037°, respectively.

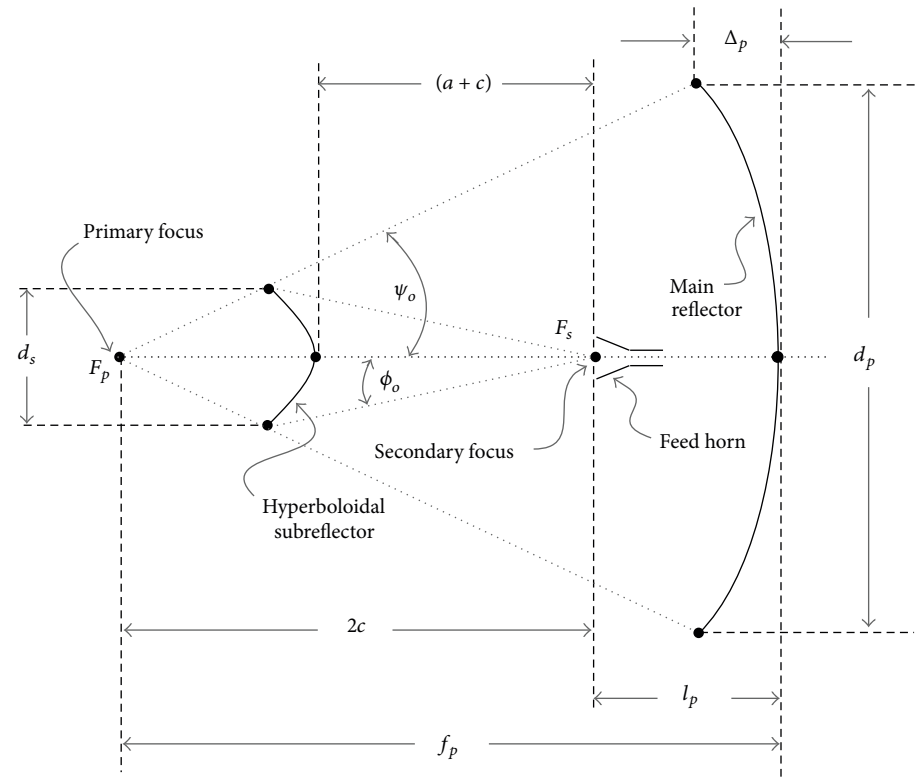


Figure 1: Geometry of a Cassegrain antenna.

Some of these parameter values are selected from standard values. The other parameters are found using geometrical relations found in literature [3, 14].

It is assumed that the feed antenna is located at the origin and direction of feed radiation is towards the negative $z$ axis. So the hyperboloid must be located at the negative side of the $z$ axis. One of the focuses of the hyperboloid must be at origin so that it coincides with the feed. The equation of such a hyperboloidal surface symmetric around the $z$ axis is given by the following equation [15]:

$$\frac{(z+c)^2}{a^2} - \frac{x^2+y^2}{b^2} = 1, \tag{1}$$

where

$$b^2 = c^2 - a^2. \tag{2}$$

The parameters $a$ and $c$ are related to the position of the vertex and focus of the hyperboloid as shown in Figure 1 [15]. The parameter $\rho_s$ is defined as the radius of surface point projected on the $xy$ plane. It is related to $x$ and $y$ by

$$\rho_s^2 = x^2 + y^2. \tag{3}$$

Equation (1) can be modified as

$$\frac{(z+c)^2}{a^2} - \frac{\rho_s^2}{b^2} = 1, \tag{4}$$

$$z = -c - \frac{a}{b}\sqrt{b^2 + \rho_s^2}. \tag{5}$$

In (5), the negative square root is taken because the defined coordinate system places the hyperboloid in the negative $z$ axis.

For a circularly symmetric shaped subreflector, (4) and, correspondingly, (5) need be modified. A distortion function, $\delta(\cdot)$, is introduced in the equations to get the shaped surface:

$$\frac{(z+c)^2}{a^2} - \frac{\rho_s^2}{b^2}\delta(\rho_s) = 1, \tag{6}$$

$$z = -c - \frac{a}{b}\sqrt{b^2 + \rho_s^2\delta(\rho_s)}. \tag{7}$$

The distortion function, $\delta(\cdot)$, must be a function of $\rho_s$ to maintain circular symmetry. The shape of the surface depends on the expression of $\delta(\cdot)$. Through literature review, it is found that shaped hyperboloidal subreflectors are usually different from unshaped hyperboloids near the edges [13]. The shaped surface curves towards the vertex at the edges. An exponential function with arguments containing even powers of $\rho_s$ can give the desired shaped. The following generalized expression of the distortion function is developed:

$$\delta(\rho_s) = \exp\left(\sum_{n=1}^{N} \tau_n \rho_s^{2n\zeta_n}\right). \tag{8}$$

The function contains $2N$ number of parameters denoted by $\tau_n$ and $\zeta_n$. Here, $\tau_n$ denotes the $n$th amplitude distortion parameter and $\zeta_n$ denotes the $n$th exponent distortion parameter. The parameters together are termed distortion parameters.

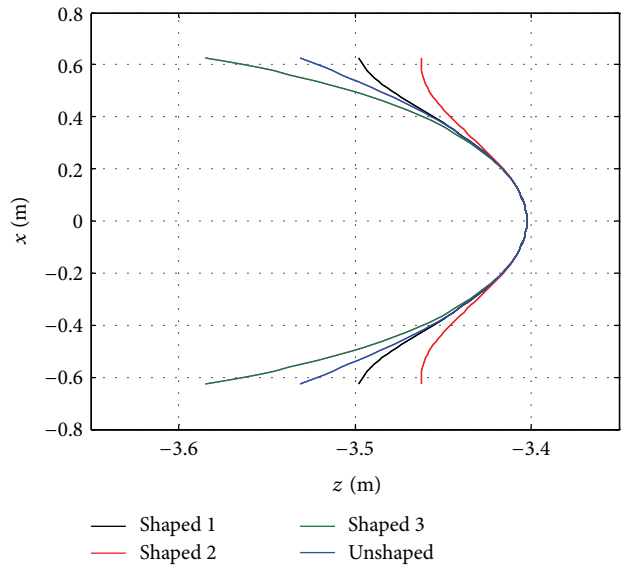


FIGURE 2: Multiple shaped subreflectors generated by using different sets of distortion parameter values.

For high values of $N$, the control over the curvature of the surface is more precise. But it increases the number of parameters required to define the surface. It is found that, for practical subreflector surfaces, $N = 2$ is sufficient and only 4 parameters are required to define the surface.

Two-dimensional and three-dimensional representations of shaped surfaces obtained using (7) are shown in Figures 2 and 3. The figures are generated using arbitrary values of the distortion parameters. However, it is necessary to establish that practical shaped subreflector surfaces can be accurately represented by these equations. Practical data of a shaped hyperboloidal and subreflector surfaces are taken from literature [13]. The dimensions are normalized with respect to subreflector diameter in [13]. By adjusting the distortion parameters in (8) and using them in (7), a surface closely resembling the shaped subreflector surface of [13] is generated. The results are shown in Figure 4.

It is clear that the unshaped surface is very different from the shaped surface. With $\tau_1 = -3.3363$, $\zeta_1 = 0.5706$, $\tau_2 = 2.1697$, and $\zeta_2 = 0.1951$, the sum of squares of the error between the defined shaped hyperboloidal surface and the practical data of [13] is only $3.2 \times 10^{-5}$. So the derived equations represent the practical shaped surface very closely.

*2.2. Differential Geometric Analysis.* The design procedures of reflector antennas are interrelated with the numerical techniques that are used to analyse those antennas. GO and UTD are two common numerical techniques employed for these purposes. To apply these methods, it is necessary that the reflecting surfaces be expressed in differential geometric form. Also, the normal vector at each point of the surface must also be defined to compute scattered field using GO or UTD method [16, 17].

The shaped hyperboloidal surface defined by (7) can be represented using parameters $\rho_s$ and $\phi_s$ in differential geometrical form as [16, 18]

$$\mathbf{r} = \rho_s \cos\phi_s \hat{\mathbf{x}} + \rho_s \sin\phi_s \hat{\mathbf{y}} - \left[c + \frac{a}{b}\sqrt{b^2 + \rho_s^2 \delta(\rho_s)}\right]\hat{\mathbf{z}}. \quad (9)$$

Here, $(\rho_s, \phi_s)$ are the polar coordinates of the projection of a surface point on the $xy$ plane. The unit normal vector, $\hat{\mathbf{n}}_\mathbf{s}$, is defined by the following equation [19]:

$$\hat{\mathbf{n}}_\mathbf{s} = \frac{(\partial\mathbf{r}/\partial\rho_s) \times (\partial\mathbf{r}/\partial\phi_s)}{\left|(\partial\mathbf{r}/\partial\rho_s) \times (\partial\mathbf{r}/\partial\phi_s)\right|}. \quad (10)$$

The differential geometrical parameters along with the coordinate system are shown in Figure 5. The incident ray vector ($\hat{\mathbf{s}}_\mathbf{i}$) and the reflected ray vector ($\hat{\mathbf{s}}_\mathbf{r}$) are also shown in Figure 5. As the unit normal vector is required for later calculations, (10) needs to be evaluated. The partial derivatives can be calculated from (9) using (8):

$$\frac{\partial\mathbf{r}}{\partial\rho_s} = \cos\phi_s\hat{\mathbf{x}} + \sin\phi_s\hat{\mathbf{y}} - \left[\frac{a}{2b}\frac{\rho_s\delta(\rho_s)\left\{\sum_{n=1}^{N}\tau_n\rho^{2n\zeta_n} + 2\right\}}{\sqrt{b^2 + \rho_s^2\delta(\rho_s)}}\right]\hat{\mathbf{z}}, \quad (11)$$

$$\frac{\partial\mathbf{r}}{\partial\phi_s} = -\rho_s\sin\phi_s\hat{\mathbf{x}} + \rho_s\cos\phi_s\hat{\mathbf{y}}.$$

Substituting these values in (10),

$$\hat{\mathbf{n}}_\mathbf{s} = \frac{\Lambda(\rho_s)\cos\phi_s}{\sqrt{\Lambda^2(\rho_s) + \Delta_H^2(\rho_s)}}\hat{\mathbf{x}} + \frac{\Lambda(\rho_s)\sin\phi_s}{\sqrt{\Lambda^2(\rho_s) + \Delta_H^2(\rho_s)}}\hat{\mathbf{y}} + \frac{\Delta_H(\rho_s)}{\sqrt{\Lambda^2(\rho_s) + \Delta_H^2(\rho_s)}}\hat{\mathbf{z}}, \quad (12)$$

where

$$\Delta_H(\rho_s) = 2b\sqrt{b^2 + \rho_s^2\delta(\rho_s)},$$
$$\Lambda(\rho_s) = a\delta(\rho_s)\varepsilon(\rho_s), \quad (13)$$
$$\varepsilon(\rho_s) = \rho_s\left\{\sum_{n=1}^{N}\tau_n\rho^{2n\zeta_n} + 2\right\}.$$

For a given set of distortion parameter values, the shaped subreflector surface and the normal vectors can be evaluated using these equations.

## 3. Synthesizing the Main Reflector

In a dual reflector system, the shape of the main reflector is completely dependent on the shape of the subreflector. Once the shape of the subreflector is defined, the main reflector must be shaped so that the path lengths of the rays are

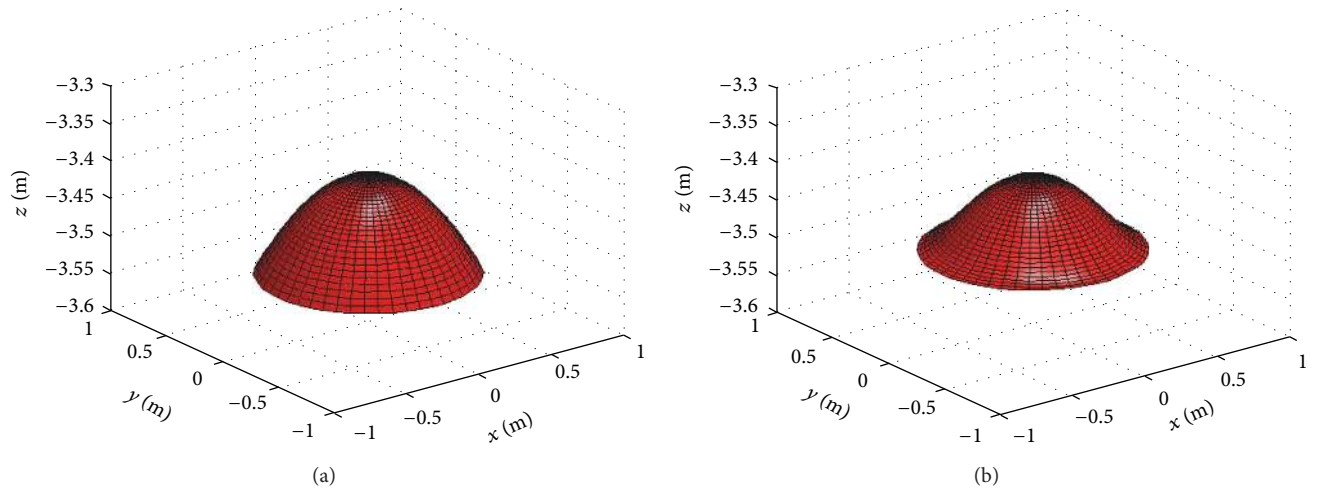


FIGURE 3: Three-dimensional representation of (a) conventional hyperboloid and (b) shaped hyperboloid.

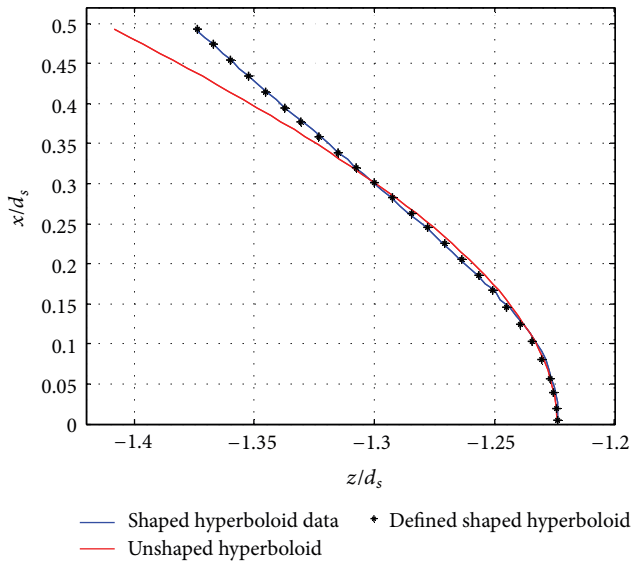


FIGURE 4: Representation of practical hyperboloidal shaped subreflector using the proposed equations.

constant at an observation plane perpendicular to the main reflector axis. Using GO methods to calculate the incident and reflected ray vectors, the required position of a point on the main reflector surface for a given point on the subreflector surface can be formulated.

The geometry of dual reflector system with a shaped hyperboloidal subreflector is shown in Figure 6. An observation plane is defined parallel to the $xy$ plane. In the two-dimensional diagram of Figure 6, the observation plane is shown as line parallel to $x$ axis going through the point $(0, 0, z_{\text{ref}})$. For a ray emitted from the feed, the sum of the distances $d_1$, $d_2$, and $d_3$ must be constant ($k_1$), irrespective of the position of reflection on the subreflector surface. So

$$d_1 + d_2 + d_3 = k_1. \tag{14}$$

The distance $k_1$ can be calculated by considering an axial ray from the feed (along the $z$ axis). From Figure 6, for the axial ray, the distance from feed to subreflector is $(a + c)$; then the distance from the subreflector to main reflector is $(a + c + l_p)$, and finally the distance from main reflector to observation point is $(l_p - z_{\text{ref}})$, when considering $z_{\text{ref}}$ to be a negative quantity. So $k_1$ is calculated as

$$\begin{aligned} k_1 &= (a + c) + \left(a + c + l_p\right) + \left(l_p - z_{\text{ref}}\right) \\ &= 2\left(a + c + l_p\right) - z_{\text{ref}}. \end{aligned} \tag{15}$$

The parameter $l_p$ can be related to the geometrical parameters of the unshaped subreflector, $c$, and the unshaped main reflector $f_p$ as seen in Figure 6:

$$l_p = f_p - 2c. \tag{16}$$

Using (16) in (15),

$$k_1 = 2\left(a - c + f_p\right) - z_{\text{ref}}. \tag{17}$$

The distance $d_1$ is related to the coordinates of the subreflector surface point $(x_s, y_s, z_s)$ as

$$d_1 = \sqrt{x_s^2 + y_s^2 + z_s^2}. \tag{18}$$

The reflected ray from the main reflector is parallel to the z axis. The distance $d_3$ can easily be related to the coordinates of the main reflector surface point $(x_m, y_m, z_m)$ as

$$d_3 = z_m - z_{\text{ref}}. \tag{19}$$

To calculate distance $d_2$, it is necessary to calculate the reflected ray vector. The unit vector in the direction of the reflected ray is found from GO method and is given by [16]

$$\hat{\mathbf{s}}_{\mathbf{r}} = \hat{\mathbf{s}}_{\mathbf{i}} - 2\left(\hat{\mathbf{n}}_{\mathbf{s}} \cdot \hat{\mathbf{s}}_{\mathbf{i}}\right)\hat{\mathbf{n}}_{\mathbf{s}}, \tag{20}$$

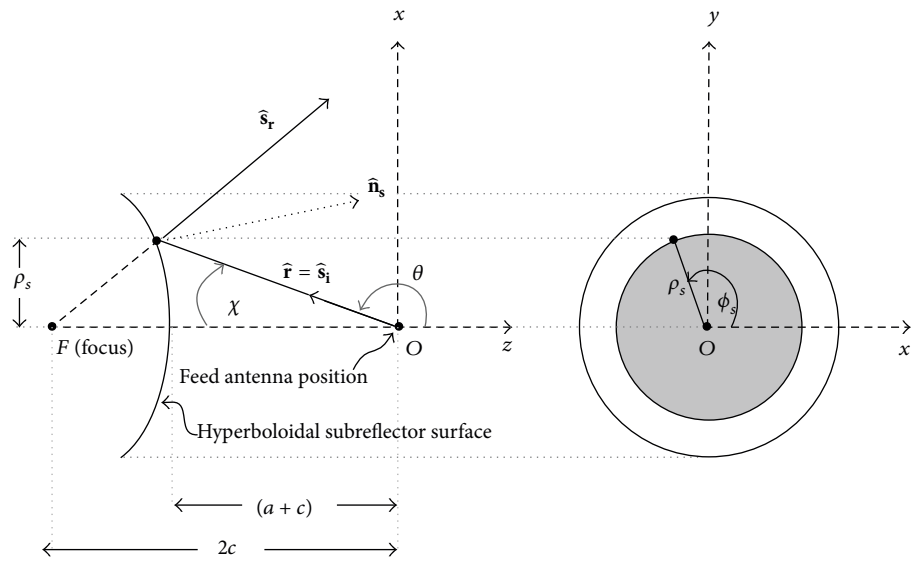


Figure 5: Differential geometric representation of the shaped hyperboloidal subreflector.

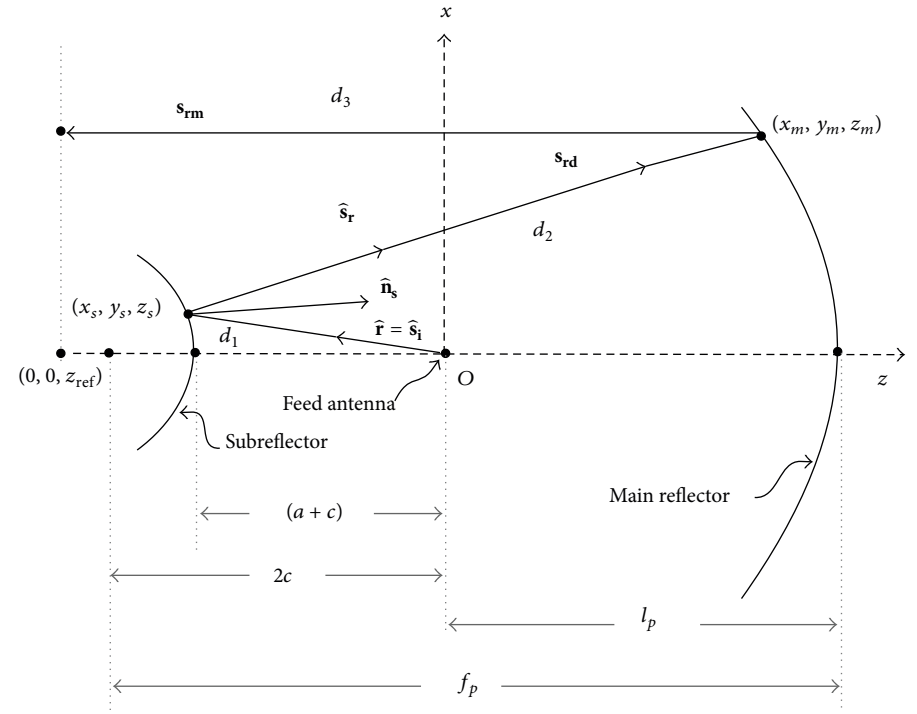


Figure 6: Synthesis of main reflector surface for a given shaped subreflector.

where

$$\hat{\mathbf{s}}_\mathbf{i} = \hat{\mathbf{r}} = \frac{\mathbf{r}}{|\mathbf{r}|}. \tag{21}$$

The vector $\mathbf{r}$ is defined by (9) and $\hat{\mathbf{n}}_\mathbf{s}$ is defined by (12). Once the unit vector along the reflected ray is formulated, the reflected ray vector, $\mathbf{s_{rd}}$, defined from the reflection point on the subreflector surface can be defined as

$$\mathbf{s_{rd}} = \hat{\mathbf{s}}_\mathbf{r} d_2 + x_s \hat{\mathbf{x}} + y_s \hat{\mathbf{y}} + z_s \hat{\mathbf{z}}. \tag{22}$$

In (22), the subreflector surface point vector appears as additive term. This term is used to shift the vector from origin to the subreflector surface point $(x_s, y_s, z_s)$.

Equation (22) can be reorganized as

$$\begin{aligned}\mathbf{s_{rd}} = {} & \left\{\left(\hat{\mathbf{s}}_\mathbf{r} \cdot \hat{\mathbf{x}}\right) d_2 + x_s\right\} \hat{\mathbf{x}} + \left\{\left(\hat{\mathbf{s}}_\mathbf{r} \cdot \hat{\mathbf{y}}\right) d_2 + y_s\right\} \hat{\mathbf{y}} \\ & + \left\{\left(\hat{\mathbf{s}}_\mathbf{r} \cdot \hat{\mathbf{z}}\right) d_2 + z_s\right\} \hat{\mathbf{z}}.\end{aligned} \tag{23}$$

The components of this vector indicate the coordinates of the main reflector [18, 19]. So

$$x_m = (\hat{\mathbf{s}}_\mathbf{r} \cdot \hat{\mathbf{x}})\, d_2 + x_s,$$
$$y_m = (\hat{\mathbf{s}}_\mathbf{r} \cdot \hat{\mathbf{y}})\, d_2 + y_s, \quad (24)$$
$$z_m = (\hat{\mathbf{s}}_\mathbf{r} \cdot \hat{\mathbf{z}})\, d_2 + z_s.$$

Substituting the value of $z_m$ from (24) to (19),

$$d_3 = (\hat{\mathbf{s}}_\mathbf{r} \cdot \hat{\mathbf{z}})\, d_2 + z_s - z_{\text{ref}}. \quad (25)$$

Now, using (18) and (25) in (14) and solving for $d_2$,

$$d_2 = \frac{2\left(a - c + f_p\right) - \sqrt{x_s^2 + y_s^2 + z_s^2} - z_s}{1 + (\hat{\mathbf{s}}_\mathbf{r} \cdot \hat{\mathbf{z}})}. \quad (26)$$

Equation (26) can be used to calculate $d_2$ for a given subreflector surface point and it can be replaced in (24) to calculate corresponding main reflector surface point. Thus, the derived equations can synthesize the main reflector surface for an arbitrary subreflector surface.

To verify the method, the main reflector for an unshaped hyperboloid is synthesized. It is found that the synthesized main reflector is an exact paraboloid, which is expected. Thus, the method is verified.

## 4. Numerical Example

For numerical analysis, the feed is assumed to be a conical corrugated horn antenna. The radiated field from the horn is calculated using standard equations [1]. The fields scattered from the subreflector are calculated using UTD method. The observation points are taken on the main reflector surface. First, the scattered field from an unshaped hyperboloid is calculated. The results are shown in Figure 7. The rapid fall of the reflected field indicates the reflection shadow boundary (RSB) of the subreflector [16]. It can be observed from Figure 7 that the scattered field tapers gradually as the observation angle increases. This creates a tapered illumination of the main reflector. Using the proposed method, a shaped hyperboloidal subreflector is defined which produces a more uniform field distribution. An optimization algorithm can be used to find the optimum set of distortion parameter values that will create a subreflector surface that will create a desired illumination. The scattered field for a shaped subreflector defined by the parameters $\tau_1 = -3.3928$, $\tau_2 = 2.5015$, $\zeta_1 = 1.7212$, and $\zeta_2 = 0.7184$ is shown in Figure 8. The values of the distortion parameters are calculated using differential evolution (DE) optimization algorithm [20–22]. The fitness function in the optimization process is defined in terms of uniformity of the scattered field. As a result, the algorithm converges to a set of distortion parameter values that result in a uniform aperture distribution. It can be observed that the scattered field is more uniform when the subreflector is shaped.

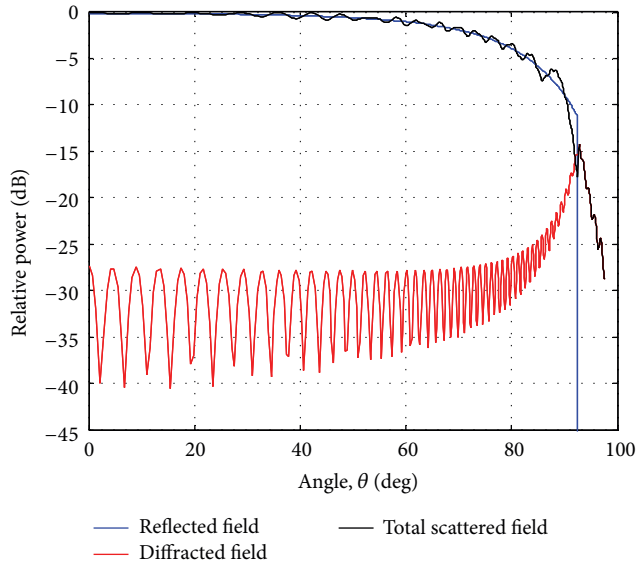


Figure 7: Scattered field from an unshaped hyperboloidal subreflector.

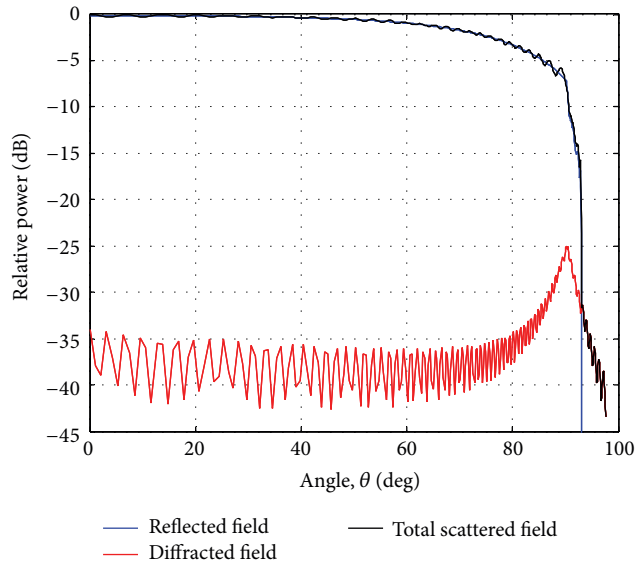


Figure 8: Scattered field from a shaped hyperboloidal subreflector.

## 5. Conclusion

A novel method of expressing the shaped reflector surfaces has been presented in this paper. The method expresses the shaped subreflector surface as distorted form of the unshaped conventional conic surface. This allows us to mathematically express the shaped subreflector surface with only a few parameters. The shaped main reflector surface is synthesized employing GO method and using the derived equation of the shaped subreflector. A numerical example is provided to show how a shaped reflector system defined by the proposed method can create a uniform field distribution over the main reflector aperture. As only a few parameters completely

describe the shaped reflector surfaces, the computational burden of design and optimization process of shaped reflectors can be reduced using the proposed method.

## Conflict of Interests

The authors declare that there is no conflict of interests regarding the publication of this paper.

## References


[1] J. L. Volakis, Ed., *Antenna Engineering Handbook*, McGraw-Hill, 4th edition, 2007.

[2] C. A. Balanis, Ed., *Modern Antenna Handbook*, John Wiley & Sons, New York, NY, USA, 2008.

[3] J. W. M. Baars, *The Paraboloidal Reflector Antenna in Radio Astronomy and Communications: Theory and Practice*, Springer, 2007.

[4] W. L. Stutzman and G. A. Thiele, *Antenna Theory and Design*, John-Wiley & Sons, 1981.

[5] S. Silver, Ed., *Microwave Antenna Theory and Design*, McGraw-Hill, New York, NY, USA, 1st edition, 1949.

[6] V. Galindo, "Design of dual-reflector antennas with arbitrary phase and amplitude distributions," *IEEE Transactions on Antennas and Propagation*, vol. 12, pp. 403–408, 1964.

[7] C. S. Lee, "A simple method of dual-reflector geometrical optics synthesis," *Microwave and Optical Technology Letters*, vol. 1, no. 10, pp. 367–371, 1988.

[8] Y. Rahmat-Samii and J. Mumford, "Reflector diffraction synthesis using global coefficients optimization techniques," in *Proceedings of the Antennas and Propagation Society International Symposium*, vol. 3, pp. 1166–1169, IEEE, San Jose, Calif, USA, June 1989.

[9] D.-W. Duan and Y. Rahmat-Samii, "Generalized diffraction synthesis technique for high performance reflector antennas," *IEEE Transactions on Antennas and Propagation*, vol. 43, no. 1, pp. 27–40, 1995.

[10] Y. Rahmat-Samii and V. Galindo-Israel, "Shaped reflector antenna analysis using the jacob-bessel series," *IEEE Transactions on Antennas and Propagation*, vol. 28, no. 4, pp. 425–435, 1980.

[11] Y. Kim and T.-H. Lee, "Shaped circularly symmetric dual reflector antennas by combining local conventional dual reflector systems," *IEEE Transactions on Antennas and Propagation*, vol. 57, no. 1, pp. 47–56, 2009.

[12] F. J. S. Moreira and J. R. Bergmann, "Shaping axis-symmetric dual-reflector antennas by combining conic sections," *IEEE Transactions on Antennas and Propagation*, vol. 59, no. 3, pp. 1042–1046, 2011.

[13] M. S. Narasimhan, P. Ramanujam, and K. Raghavan, "GTD analysis of the radiation patterns of a shaped subreflector," *IEEE Transactions on Antennas and Propagation*, vol. 29, no. 5, pp. 792–795, 1981.

[14] C. Granet, "Designing axially symmetric cassegrain or gregorian dual-reflector antennas from combinations of prescribed geometric parameters," *IEEE Antennas and Propagation Magazine*, vol. 40, no. 2, pp. 76–81, 1998.

[15] A. D. Polyanin and A. V. Manzhirov, *Handbook of Mathematics for Engineers and Scientists*, Chapman & Hall/CRC, Taylor & Francis, 2007.

[16] D. A. McNamara, C. W. I. Pistorius, and J. A. G. Malherbe, *Introduction to the Uniform Geometrical Theory of Diffraction*, Artech House, London, UK, 1990.

[17] K. Lim, H. Ryu, and J. Choi, "UTD analysis of a shaped subreflector in a dual offset-reflector antenna system," *IEEE Transactions on Antennas and Propagation*, vol. 46, no. 10, pp. 1555–1559, 1998.

[18] B. O'Niell, *Elementary Differential Geometry*, Academic Press, Elsevier, 2nd edition, 2006.

[19] D. V. Widder, *Advanced Calculus*, Prentice-Hall, New Delhi, India, 2nd edition, 2004.

[20] R. Storn and K. Price, "Differential evolution—a simple and efficient heuristic for global optimization over continuous spaces," *Journal of Global Optimization*, vol. 11, no. 4, pp. 341–359, 1997.

[21] K. V. Price, R. M. Storn, and J. A. Lampinen, *Differential Evolution: A Practical Approach to Global Optimization*, Springer, 2005.

[22] A. Qing and C. K. Lee, *Differential Evolution in Electromagnetics*, Springer, Berlin, Germany, 2010.